Accepted Manuscript

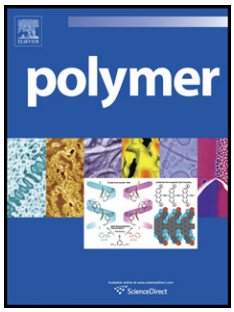

Evaluation of photo-induced crosslinking of thymine polymers using FT-IR spectroscopy and chemometric analysis

Santiago A. Bortolato, Katelyn E. Thomas, Kristin McDonough, Richard W. Gurney, Débora M. Martino

PII: S0032-3861(12)00764-1

DOI: 10.1016/j.polymer.2012.09.007

Reference: JPOL 15665

To appear in: *Polymer*

Received Date: 24 August 2012

Accepted Date: 1 September 2012

Please cite this article as: Bortolato SA, Thomas KE, McDonough K, Gurney RW, Martino DM, Evaluation of photo-induced crosslinking of thymine polymers using FT-IR spectroscopy and chemometric analysis, *Polymer* (2012), doi: 10.1016/j.polymer.2012.09.007.

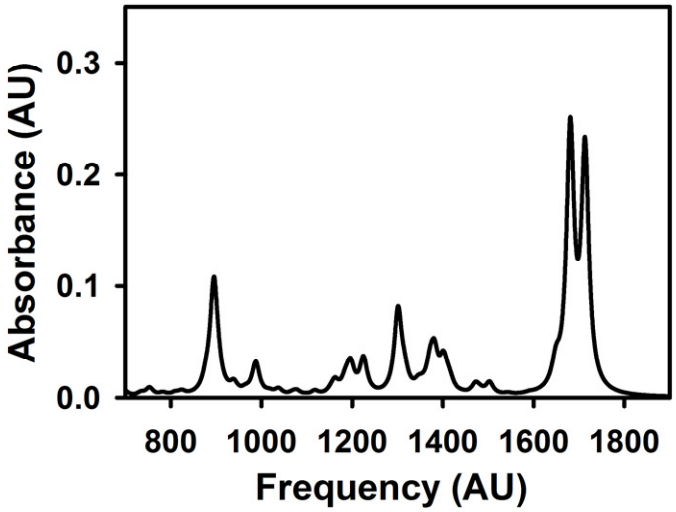

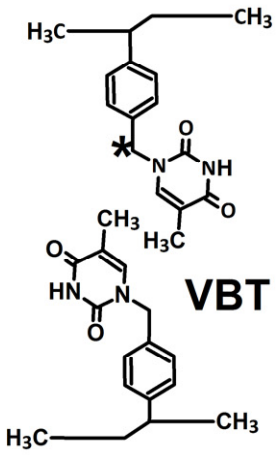

Evaluation of photo-induced crosslinking of thymine polymers using FT-IR spectroscopy and chemometric analysis

Santiago A. Bortolato[1], *Katelyn E. Thomas*[2], *Kristin McDonough*[2], *Richard W. Gurney*[2*], *Débora M. Martino*[1]

[1] Instituto de Desarrollo Tecnológico para la Industria Química (INTEC) (UNL -CONICET) Güemes 3450, S3000GLN Santa Fe, Argentina.

[2] Department of Chemistry and Physics Simmons College 300 The Fenway, Boston, MA, 02115, USA.

* Corresponding author. Address: Department of Chemistry and Physics Simmons College 300 The Fenway, Boston, MA, 02115, USA.. Tel: +01.617.521.2729. Fax: ++01.617.521.3086. E-mail: richard.gurney@simmons.edu.

ABSTRACT

The photo-induced immobilization of 4-vinylbenzyl thymine (VBT) and 4-vinylbenzyl triethyl ammonium chloride (VBA) copolymers has been investigated with the aid of grazing-angle specular-reflectance FT-IR spectroscopy. As irradiation time increases, changes in the structure of pendant thymine groups in the copolymer due to the crosslinking process result in shifts of the copolymer network's vibrational frequencies, as well as changes in numerous IR band intensities. In this work, chemometric methods have been applied to the FTIR data obtained while monitoring the time evolution of curing of VBT-VBA copolymers of varying composition. The spectral data obtained with FT-IR normally provide information only about the degree of conversion of the reactants in the final product but there is no knowledge about how many compounds are involved or how they evolve over time. The use of the so-called Multivariate Curve Resolution-Alternating Least Squares allows the sequential estimation of the contribution to the signal due to the different species in the matrix data.

Keywords: Biopolymers, VBT, FTIR spectroscopy, Multivariate analysis.

1. INTRODUCTION

Nature has synthesized abundant, well-designed and inspirational materials in terms of green chemistry, especially in respect to atom economy and energy utilization. Through the identification of these naturally occurring green mechanisms novel materials have been developed. The study of bio-inspired functional polymers containing reactive moieties had grown enormously in last few years as a consequence of the environmental and toxicological problems linked to the synthesis and non-degradability of traditional plastics. During the last decade, extensive research has particularly focused on the design of synthetic polymers containing nucleic acid bases, which are appealing due to their capacity to combine the advantages of synthetic functional polymers, while simultaneously exhibiting interesting supramolecular properties found in nature [1].

Scientists have exploited the chemistry of the [2π + 2π] photo-dimerization of thymine base units of DNA in the presence of UV light (λ ~ 280 nm) via the incorporation of pendant thymine groups onto synthetic polymer backbones [2]. A novel highly multifunctional green monomer, 4-vinylbenzyl thymine (VBT) has been developed [3-6]. The synthesis of polymers containing VBT acquired particular significance and had opened the possibility of producing a wide variety of polymers. These environmentally benign polymers are based on a polystyrene (PS) backbone, and since the VBT homopolymer is water insoluble due to strong intermolecular interactions, the introduction of charged functional groups such as 4-vinylbenzyl triethylammonium chloride (VBA) allows for the processing of the polymer in water, eliminating the need of toxic solvents (Scheme 1).

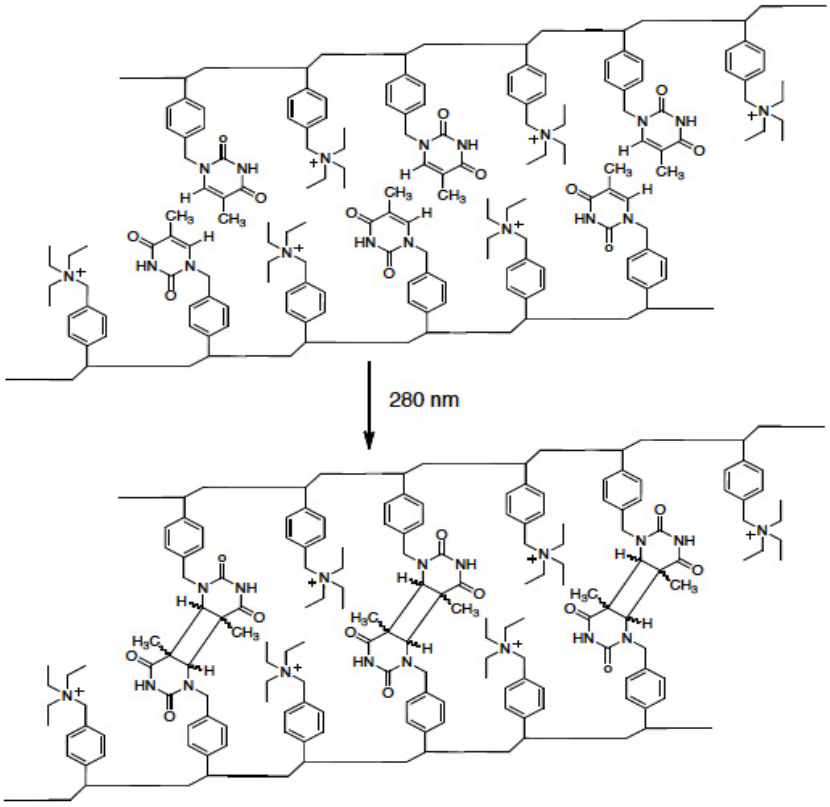

Scheme 1

Exposure to low levels of UV light (λ ~ 280 nm) induces a dimerization reaction between adjacent thymine moieties and generates covalent cyclobutane dimers resulting in the crosslinking of polymer chains, and therefore, a decrease in the solubility of thymine containing polymers (Scheme 1). In the initial presence of UV light, the photo-crosslinking of VBT copolymers and consequent increase in the average molecular weight does not affect solubility. As the irradiation dose increases, the degree of crosslinking increases and the copolymer undergoes a transition from individual polymer chains to a crosslinked network. After reaching a certain threshold, the 'gel point', the polymer becomes insoluble due to the high molecular weight and the complex structure of the resulting network. The selection of the correct irradiation dose would allow for the fine-tuning of polymer solubility for a specific target application. Moreover, the dimerization of thymine can be reversed, either enzymatically or by irradiation with UV light (at λ ~ 240 nm) [7]. Whitfield *et al.* demonstrated that the enzyme DNA photolyase is able to reverse the photocrosslinking in thymine containing styrene derivatives [8],

after which the polymer becomes soluble again and can be reused for subsequent applications, providing exciting opportunities to create fully recyclable materials.

The adaptability of VBT-VBA copolymers makes these materials very attractive due to the tuneability of the photo-reactivity, solubility and noncovalent interactions. The copolymer's ability to transition from individual polymeric chains to a crosslinked network allows for the modification of the polymer's physical properties, such as elasticity, tensile strength, and solubility. These properties provide an exciting wide variety of practical applications for the copolymer including antibacterial-coated surfaces [9], hair care products [10], printed circuit boards and photo-imaging systems [11-14], as well as controlled release systems for pharmaceutical and agricultural use [15-17].

Several studies related to the synthesis and the curing processes of thymine-based VBT-VBA polymers have been published. In Casis *et al.* the synthesis of VBT-VBA polymers in solution at low temperatures (65ºC) was theoretically and experimentally studied [18]. A mathematical model for the free radical copolymerization of VBT-VBA was developed, that allows the prediction of global variables (conversion, composition) and the molecular structure (molecular weight distribution and chemical composition) of the copolymers along the reaction. Barbarini *et al.* [19] investigated the photo-induced UV curing kinetics of VBT-VBA copolymers from the UV absorption spectra measured along the process. The inmobilization point (related to the gel point) was determined following the evolution of the absorbance peaks of the copolymer solution after UV irradiation. The kinetics of the crosslinking reaction was estimated from the evolution of the thymine concentration before the immobilization point considering additive contributions of repetitive unit absorbances of VBT and VBA. Differences in the kinetic constants were found for mixtures with different VBT-VBA ratios, due to the variations in the film characteristics. However, the presence of other compounds that might be generated in the reaction medium while irradiating was not considered. Bortolato *et al.* [20] studied the curing process of the copolymer VBT-VBA using UV-vis spectroscopy in combination with a Multivariate Curve Resolution Algorithm assisted by alternating least squares (MCR-ALS) chemometric model, obtaining a more accurate characterization of the evolution of the cross-linking process. The curing process of the copolymer VBT-VBA was determined to involve three species, which absorb in the spectral region analyzed. Additionally, the study allowed the evaluation of the consistency of the

chemometric decomposition obtaining a reasonable correlation between the frequency spectra and the time evolutions obtained with the algorithm.

Fourier transform infrared spectroscopy (FT-IR) provides a unique opportunity to study chemical changes based on the complexity and specificity of the infrared spectrum [21,22]. Major functional groups, that have changes associated to the reaction process, have well defined wavenumber positions and shapes in the IR spectral range. Along the reaction, the system´s properties change, and the disappearance and formation of the species can be directly monitored. These characteristics can be used to provide detailed and relevant information on reaction kinetics and mechanisms in real time, which is crucial to control the quality of the final products. The study of crosslinking has been successfully carried out on polymers including poly(cinamoylphenyl acrylate), poly(meth)acrylates as well as β-2-bromo-trans-cinnamic acid crystals [23]. However, samples of complex composition might present several difficulties to discriminate signals of interest, either due to spectral overlap or due to unknown interactions. The spectral data obtained with FT-IR normally provides information only about the degree of conversion of the reactants in the final product but there is no knowledge about how many compounds are involved or how they evolve over time [24,25]

In spite of the diverse nature of the complex systems analyzed, in many cases variations in their related experimental outputs can be expressed as a simple composition-weighted linear additive model of pure responses, with a single term per component contribution. This goal can be achieved by using chemometric methods [26]. In general, the information related to individual contributions involved in the processes cannot be drawn in a straightforward way from the raw measurements. The general idea of all chemometric methods is to fill out such areas and to provide the model of individual component contributions using exclusively the raw experimental measurements. Chemometric methods are effective tactics with little requirements; none of the pure components in a system need to be known in advance, and any information available about the system can be used [26]. In the last two decades, these tools have been widely used to solve problems of broad physical-chemical nature [27]. Specifically, in the polymer research field Hamerton *et al.* used NIR spectroscopy together with chemometric analysis to investigate different properties of cured cyanate ester/bismaleimide blends [28]. Alternatively, Scherzer *et al.* combine NIR and FTIR with chemometric methods to monitor the conversion of double bonds in acrylate coatings after irradiation whit UV light [29]. In addition, Harris and Alam

applied chemometric analysis to the ^{13}C NMR spectra to obtain information about both dynamics and morphology in of crosslinked polyolefin materials [30].

In particular, a very convenient method applied to spectroscopic data monitoring curing reactions is the Multivariate Curve Resolution Algorithm assisted by alternating least squares (MCR-ALS) [31]. The minor necessities required to apply MCR-ALS have promoted the use of resolution methods to address many chemical problems that could not be solved otherwise [32]. Similar to the kind of experiments carried out in this work, Larrechi *et al*. used MCR-ALS to analyze FTIR data and obtained representative spectra of the compounds that participate in the curing reaction between diglycidyl ether of bisphenol A and γ-valerolactone [24]. On the other hand, Larrechi and Rius showed the use of MCR-ALS to study the curing reactions of epoxy resins obtaining the concentration profiles as a function of time for the chemical species involved in the reaction and the corresponding spectra [33]. Interestingly, Garrido et al. developed a model of the curing reaction between phenyl glycidyl ether (PGE) and aniline as the curing agent, the process was studied isothermally and monitored in situ by near-infrared spectroscopy (NIR) [34]. Furthermore, these authors validated the concentration profiles obtained by combining NIR/MCR-ALS for the reaction between PGE and aniline, using high performance liquid chromatography (HPLC) as a reference method [35]. In addition, Garrido *et al*. performed a comprehensive review of the multiple posibilities of the MCR-ALS algorithm to resolve different chemical reactions using data generated by different analytical techniques such as UV-vis, NIR, FT-IR, Fluorescence, Fluorescence Resonance Energy Transfer (FRET), Nuclear Magnetic Resonance (NMR), Circular Dichroism (CD) and Raman [36].

The only essential requirement necessary to use MCR-ALS is that the experimental data matrix (matrix of intensities of response), usually called $\boldsymbol{D}$, needs to be expressed as the product of a concentration matrix by another matrix containing the raw signal of the existing species, $\boldsymbol{G}$ and $\boldsymbol{S}$ respectively [37]. Most spectroscopic techniques fulfilled this condition if the Beer-Lambert law is satisfied. Consequently, the evolution of each species that occurs in the process and the corresponding pure spectra can be determined by decomposing a data matrix generated during the monitoring of a crosslinking reaction.

Herein, the photo-induced crosslinking kinetics of VBT-VBA copolymer is determined combining FT-IR spectroscopy and a MCR-ALS chemometric model. Following the changes on the carbonyl IR peak associated to the thymine moiety, the crosslinking reaction can be

monitored. Both, simulated and experimental, systems are analyzed to show the capability of the method to determine the species and kinetics profiles present in the photo-induced crosslinking reaction. From the best of our knowledge, the use of MCR-ALS applied to IR spectroscopical data to study **photo-induced curing reactions** has not being reported. Furthermore, the method proposed here could be a competitive alternative compared to traditional techniques to determine the concentrations of the species involved in the curing reaction, having the added advantages of reduced analysis times, no sample pretreatment, no necessity of sophisticated equipment, no use of toxic solvents, among others [35] A simulated kinetic system was first analyzed to test the reliability of the implemented model. Subsequently, an experimental study of the effect of polymer composition as well as irradiation dose on the crosslinking of VBT copolymer films on reflective substrates using FT-IR spectroscopy is presented. To this effect, copolymer mixtures of different VBT-VBA composition were irradiated at 254 nm for different times and the IR spectra in the region of 400 - 4000 cm^{-1} was recorded at each interval. Finally, the total signal of each FT-IR absorption spectra was decomposed into the contribution of individual species via the chemometric algorithm, which might allow characterizing the kinetics of the curing process in particular to obtain the kinetic constant.

2. THEORY

2.1. Chemometric Analysis

MCR-ALS has been discussed in detail in previous works [26,31,37], therefore only a brief description is presented here. In this study, MCR-ALS was used to mathematically decompose the total signal of each FT-IR absorption spectra into the contribution of individual species, to quantify the content of each component in these spectra.

In the MCR-ALS multivariate method, a data matrix $\boldsymbol{D}$ is created from the experimental data. The first step of the algorithm is to express $\boldsymbol{D}$ as the product of a concentration matrix by another matrix containing the raw signal of the existing species. The bilinear decomposition for the data matrix is performed using the following equation:

$$\boldsymbol{D}_{\mathrm{JxK}} = \boldsymbol{G}_{\mathrm{JxN}}\, \boldsymbol{S}^{T}_{\mathrm{NxK}} + \boldsymbol{E}_{\mathrm{JxK}} \qquad (1)$$

where the J rows of $\boldsymbol{D}$ contain the spectra measured for different samples at each time K. The columns of $\boldsymbol{G}$ contain the temporal profiles of the N species involved in all the experiments and the columns of $\boldsymbol{S}$ represent the spectra related to these species. Finally $\boldsymbol{E}$ is the matrix of the

residuals not adjusted by the bilinear decomposition. In the analyzed cases, the matrix ***D*** had the following dimensions 623 [frequency from 700 cm^{-1} to 1900 cm^{-1}] x 39 [irradiation times].

The decomposition of ***D*** is accomplished through an iterative minimization procedure by alternating least squares of the Frobenius norm of ***E***. The minimization is initiated by providing estimated spectra for the different spectral components that are used to estimate ***G*** as follows:

$$\hat{\boldsymbol{G}} = \boldsymbol{D}(\boldsymbol{S}^T)^+ \quad (2)$$

where the symbol "^" indicates that it is a matrix estimated from Eq. (1), the superscript T means matrix transposition and the superscript "+" the generalized inverse. From □, and the original data matrix ***D***, the spectral matrix ***S*** is recalculated by the least squares

$$\hat{\boldsymbol{S}} = \boldsymbol{D}^T\left(\hat{\boldsymbol{G}}^+\right)^T \quad (3)$$

E is obtained from Eq. (1) using ***D*** and the estimated matrices □ and □. These steps are repeated until the convergence is reached. The algorithm is fitted with initial restrictions to achieve greater convergence throughout the process. The system is required to be non-negative in two dimensions, both in the irradiation time direction and in the wavelength direction.

The MCR-ALS algorithm requires the exact number of factors responsible for the analytical signal to be known, and that the system is preferably initialized with the profiles of the components as close as possible to the final result. The number of factors is estimated using principal component analysis based on singular value decomposition of the matrix ***D*** [38], the spectra of the species can be obtained from the analysis of the so called "pure" spectra, based on the method SIMPLISMA (*SIMPLe Interactive Self-modeling Mixture Analysis*), an algorithm of multivariate resolution that extracts pure spectra from mixtures of variable composition [39]. After the MCR-ALS decomposition of the ***D*** matrix is obtained, the information contained in ***G*** can be used to estimate the individual contributions of each species to the absorbance measured at each time. ***S*** contains the spectra of the different components, which are of great interest to understand how the curing process evolves.

2.2. Simulated data

To analyze the feasibility of the implemented MCR-ALS model, a set of simulated samples emulating the curing process of copolymers (A:N) was prepared. The simulated data mimic the photo-dimerization reaction as experimentally recorded when running absorbance measurements

with FTIR detection. The data simulation was performed for two main reasons. First, to understand the underlying principles that control the experimental kinetics of the analyzed systems, and second, to test the performance of the MCR-ALS algorithm in systems with a large number of relevant analytical difficulties, such as large spectral overlap and linear dependence between the compounds. These problems generate a decrease in the performance of the chosen algorithm and consequently, through the simulation the best conditions for the algoritm´s applicability can be defined [26].

Four components A, B, C and N were proposed, and the data for each one were simulated assuming a kinetic system as follows:

$$2\,A \underset{k2}{\overset{k1}{\leftrightarrow}} B \xrightarrow{k3} C;$$

$$N \longrightarrow \text{non reactive}$$

Noiseless simulated frequency spectra and kinetics profiles for the four proposed components are shown in Fig. 1a and 1b, respectively, leading to data matrices of 50×195 data points.

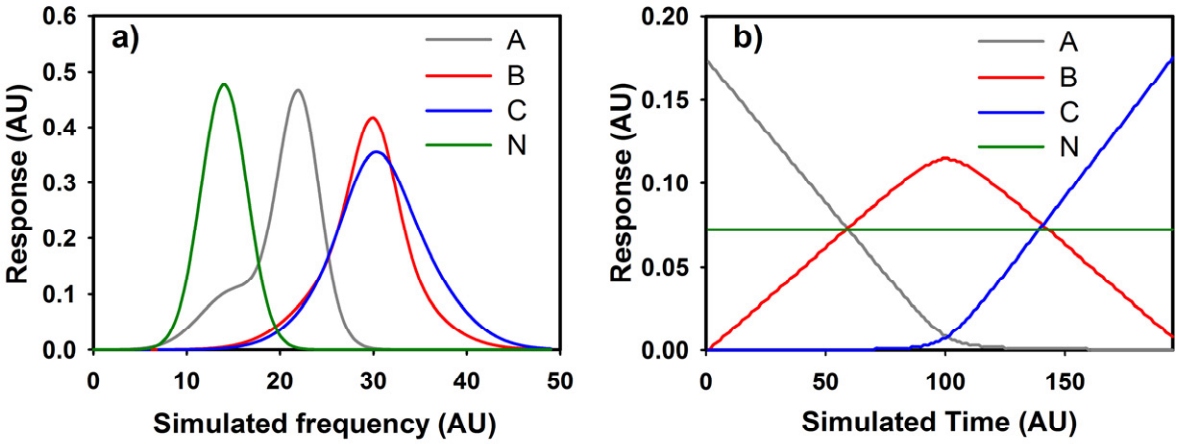

Fig. 1. Noiseless profiles for components A, B, C and N: a) Frequency mode, 50 points; b) Time mode, 195 points.

Using the analyte profiles shown in Fig. 1, three samples of different copolymer ratios were prepared: sample **1**, (A:N) (1:1); sample **2**, (A:N) (1:4); sample **3**, (A:N) (1:8). For each sample,

the signal-concentration relationship for analytes A, B, C and N is governed by the following equation:

$$\mathbf{X}_i = y_i \, \mathbf{S}_i \quad (4)$$

where $\mathbf{X}_i$ is the matrix signal at a particular concentration y_i, and $\mathbf{S}_i$ is a pure-analyte bilinear matrix given by the product of the corresponding profiles in each dimension:

$$\mathbf{S}_i = \mathbf{b}_i \, \mathbf{c}_i^T \quad (5)$$

where $\mathbf{b}_i$ and $\mathbf{c}_i$ are the (J×1) and (K×1) profiles shown in Fig. 1a and 1b, respectively, (J and K are the number of channels in each dimension) and are both normalized to the unit length. The subscript *i* corresponds to analytes A, B, C and N, respectively.

The concentrations y_i of each component are adjusted to the kinetic equations given by the proposed mechanism. Therefore, the following reaction speeds are used:

$$\begin{aligned} dy_A/dt &= -k_1 . y_A^2 + k_2 . y_B \\ dy_B/dt &= k_1 . y_A^2 - k_2 . y_B - k_3 . y_c \\ dy_C/dt &= k_3 . y_B \\ dy_N/dt &= 0 \end{aligned} \quad (6)$$

where k_i is the rate constant for analyte *i*, and the ratios used in the model are as follows: $k_1/k_2 = 1x10^3$ and $k_1/k_3 = 10$. Solving numerically the system of ordinary differential equations [Eq. (6)], the concentration values y_i for each analyte were found, and then used in Eq. (4) to generate different matrices $\mathbf{X}_i$.

To construct the simulated data, the signal for a typical sample is given by the sum of the contributions of four species:

$$\mathbf{M} = \mathbf{X}_A + \mathbf{X}_B + \mathbf{X}_C + \mathbf{X}_N \quad (7)$$

Once the noiseless matrices were obtained, gaussian noise was added to all signals. The standard deviation was 0.0015 units, representing 1% with respect to the maximum signal of each analyte at unit concentration. The data matrices were then subjected to the MCR-ALS data processing technique.

3. EXPERIMENTAL SECTION

3.1. Copolymer Synthesis and Characterization

All reagents were purchased in the purest available form and were used as received. Sodium hydroxide, isopropanol and hexanes were purchased from Fisher Scientific; 4-vinylbenzyl

chloride, hydrochloric acid, azobisisobutyronitrile, acetone, triethylamine, 2,6-di-tert-butyl-4-methylphenol and dichloromethane were purchased from Sigma Aldrich; thymine (99%) was purchased from Acros Organics, 190 proof ethanol was purchased from PHARMCOAPER. A 3,600 Mw polystyrene standard was purchased from American Polymer Standards Corp. VBT was synthesized from thymine and VBA was synthesized from vinylbenzyl chloride and triethylamine as described previously [6]. Based on ^{1}H NMR spectra and melting point results, the monomeric products were deemed pure enough for the synthesis of the polymers.

To produce water-soluble polymers, VBT was copolymerized in a free radical process with the cationic monomer, VBA. The ratio of VBT:VBA comonomers influences the behavior of the VBT polymeric system and varies depending on the application. Therefore, typical VBT_n:VBA_m ratios ranging from 1:1 through 1:8 have been synthesized.

VBT:VBA 1:1 copolymer. To a 300 mL, 3-neck, round-bottomed flask containing 200 mL isopropanol was added VBT (2.51 g, 0.0103 mol) and VBA (2.62 g, 0.0103 mol). The round-bottomed flask containing the reaction solution was sonicated at 60°C until both VBT and VBA were dissolved and the solution was clear (about an hour). Once dissolved, a stirring bar was added to the round-bottomed flask and the reaction mixture was stirred and heated to 65°C under inert N_2 atmospheric conditions. At 65°C a solution of Azobisisobutyronitrile (AIBN) (0.0477 g, $2.9x10^{-4}$ mol) dissolved in 25 mL isopropanol was added to the reaction mixture, and the reaction was kept at 65°C for 16-20 hours. Subsequently, the reaction mixture was removed from heat, cooled to room temperature and placed in an ice bath. The reaction mixture was transferred to a 500 mL single necked roundbottomed flask and was concentrated to about 50% by rotary evaporation. The resulting solution was slowly poured into a beaker containing 300 mL of acetone and stirred until a white powder precipitate crashed out of the acetone/ispropanol mixture. The resulting white solid powder was filtered twice with a coarse, glass fritted filter, washed with cold acetone and allowed to dry in the vacuum oven. To verify the absence of unreacted monomers, the precipitated polymer was analyzed by ^{1}H NMR spectroscopy (Bruker 300 MHz) and the typical vinyl group signal at chemical shifts between 5 and 6 ppm was not observed in the spectra.

VBT:VBA 1:4 and 1:8 copolymers were synthesized via identical procedures only varying the corresponding ratios of starting monomers.

3.2. Copolymer Curing: Coating Preparation, Film Irradiation and Development

Water solutions of VBT:VBA_m (m = 1, 4, 8) copolymers were distributed homogeneously on the gold coated glass slides [(1" x 3" x 0.040") with a 50 Å titanium and 1,000 Å gold - Evaporated Metal Films Corporation, Ithaca, NY] using a #3 wire-round milled coating rod (R.D. Specialties Inc., Webster NY). The films were dried at room temperature for one hour and in a vacuum oven (at 80ºC ~20 torr) for another hour to give a uniform wet thickness of 6.8 µm according to the coating rod specifications [40]. Films were protected from the light throughout the process. For the polystyrene sample, an acetone solution was distributed in similar way as described for the VBT:VBA polymers.

All polymer coated slides were irradiated with a UV hand lamp (Spectroline UL, Model ENF 260c, Spectronics Corporation Westbury, NY) at 254 nm from a distance of 1.27 cm for times ranging from 0 seconds to 270 min. This process leads to the immobilization of the polymer in response to the irradiation (photo-resist). The curing reaction due to radiation was performed at room temperature, thus these coatings can be prepared on heat sensitive materials.

The analysis of thin films and monomolecular layers has traditionally been an exceptionally challenging spectroscopic measurement due to the relatively low signals obtained from the sample. Since the photo-immobilized copolymer films of VBT are very thin, the spectroscopic characterization becomes difficult. Specular reflectance sampling at high grazing angles in FTIR is currently one of the best spectroscopic techniques for measurement of thin films and monolayers on reflective surfaces due to the enhancement of infrared signal [41]. The crosslinking was monitored by FTIR spectroscopy as a function of irradiation time (equivalent to the amount of energy delivered). FTIR spectra were collected with a DigiLab Excalibur Series FTS 3000 Spectrometer outfitted with a Pike 80 Degree Specular Reflectance Accessory (80Spec) purchased from Pike Technologies (Madison, WI). Each spectrum was recorded from 400 cm^{-1} to 4000 cm^{-1} with a resolution of 2 cm^{-1}. Triplicates of copolymer thin films of VBT-VBA were prepared and irradiated at various time intervals: 15 s, 30 s, 45 s, 60 s, 5 min, 15 min, 30 min, 45 min, 60 min, 90 min, 180 min, and 270 min (13 time points). The IR chamber was purged with N_2 before sampling to eliminate interference from CO_2 and H_2O.

For the chemometric analysis, the complete spectral region was reduced to the 700 - 1900 cm^{-1} region (623 points). Therefore, the experimental data for each copolymer composition (VBT_1:VBA_1, VBT_1:VBA_4 and VBT_1:VBA_8) run in triplicates were arranged in three matrices of size 623x39. The spectra recorded in the FTIR spectrometer were saved in ASCII format, and

transferred to a PC microprocessor based on AMD Athlon X2 Dual-Core QL-60 (1.90 GHz) for subsequent manipulation.

3.3. Software

All simulated calculations (see **Section 2.2**) were made using in-house MATLAB 7.0 routines [42], which are available from the authors upon request. The routines used for MCR-ALS were executed also in MATLAB 7.0, and are freely available on the Internet [43]. Chemometric analysis processing took less than five minutes each data matrix.

The theoretical IR spectra for all the species involved in the curing process were calculated by means of SPARTAN software [44], using Hartree-Fock 32-1G method and were corrected by a factor of 0.89.

4. RESULTS AND DISCUSSION

4.1. Simulated data

The creation of the simulated data has been described in detail in the relevant **Section 2.2**. To process the data, the first step is to create the augmented ***D*** arrays for samples **1**, **2** and **3**, which are subsequently processed by MCR-ALS [Eqs. (1)-(3)].

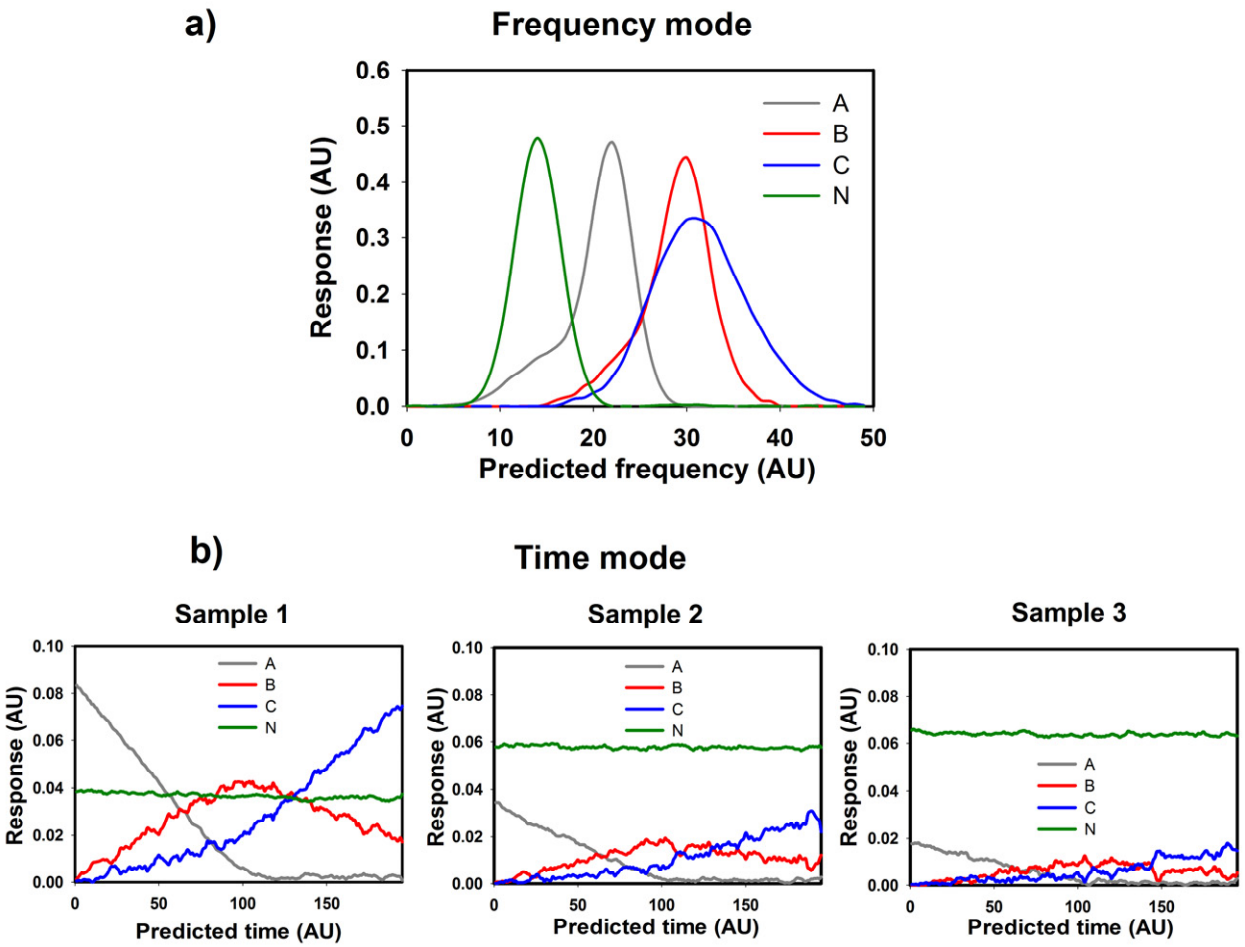

Fig. 2. a) Predicted frequency profile and b) predicted time evolution resolved by MCR-ALS for simulated samples **1**, **2** and **3**.

The MCR-ALS predicted spectral information, shown in Fig. 2a, is very similar to the simulated data, Fig. 1a. However, the MCR-ALS predicted kinetic profiles (Fig. 2b) are less satisfactory, judging from the poor signal-to-noise ratio in the temporal evolutions; especially for the components B and C. The high-level of noise is most likely due to a strong spectral overlap of these two analytes (Fig. 1a), which results from some ambiguity in the solution found by the algorithm. In addition, this effect becomes more noticeable as the concentration of the component A decreases respect to the component N, which leads to a concomitant decrease of the net signal of species B and C, making them more susceptible to the ambiguity discussed above. Despite the aforementioned problems, the algorithm was able to suitably resolve the samples, as evidenced by the correct prediction of the number of components present in the

mixture, the similarity of the MCR-ALS predicted spectra to the simulated spectra and the reasonable determination of the kinetics for each component.

In summary, the algorithm has some limitations but however the MCR-ALS analysis method is able to successfully predict the number of components, the associated kinetics and each component spectra.

4.2. Experimental data

Fig. 3 shows an overlaid spectra of a VBT:VBA (1:1) unirradiated copolymer (solid line) and a highly irradiated film (dashed line). The only IR peaks which should change during the curing reaction of thymine based copolymers are associated with the VBT units, due to changes in both structure and chemical environment linked to the formation of thymine photo-dimers.

Upon comparison of the IR experimental data of the uncrosslinked and higly crosslinked copolymer (Fig. 3) with the theoretical IR spectra calculated by Spartan (Fig. 4), there are peaks corresponding to the vibrational modes of symetrical and antisymmetrical CH stretching (~2920-2560 cm^{-1}) (not shown) and aromatic CH out of plane (oop) wagging (~790-840 cm^{-1}). These peaks can be associated solely to the polystyrene backbone, and therefore should remain unchanged after irradiation. In addition, during the crosslinking process the chemical environment of the VBA's cationic moieties remain unaltered and the IR characteristics peaks associated with N-$(CH_2$-$CH_3)_3$ wagging (~1490 cm^{-1}) and N-CH_2- wagging (~1250-1280 cm^{-1}) should also remain unchanged within the spectra.

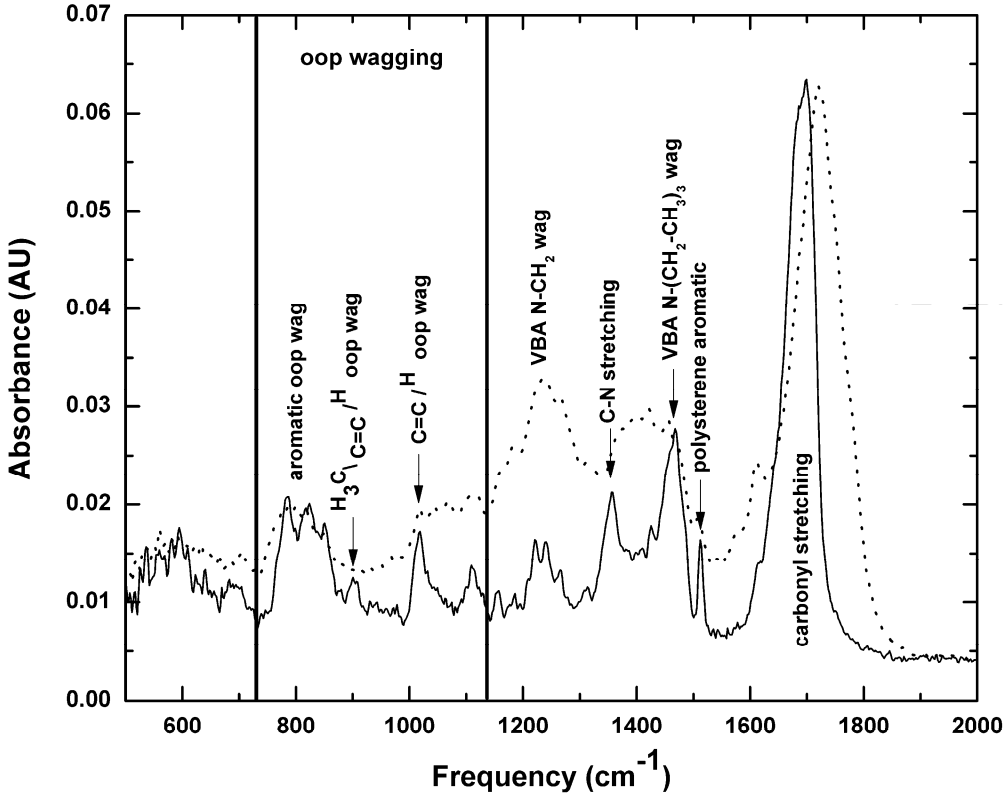

Fig. 3. Grazing angle specular reflectance FT-IR overlaid spectra of copolymer VBT:VBA 1:1 thin film on a gold coated slide: (solid line) zero irradiation time and (dashed line) 270 min irradiation time.

The thymine moeity contains two non-equivalent C=O groups, one attached to C_2 and the other attached to C_4; each contributing a unique carbonyl stretching frequency to the spectra. At zero irradiation time there are two peaks at 1684 cm^{-1} and 1700 cm^{-1}. The appearance of only one broad carbonyl peak is explained due to "an average" of all the carbonyl stretching peaks within the copolymer system at that particular irradiation time. As the curing reaction proceeds, the copolymer becomes crosslinked and the thymine moieties become dimerized resulting in the disappearance of the 5-6 carbon-carbon double bond of the pendant α,β-unsaturated amide of thymine, and the transformation into an α,β-saturated amide. FT-IR spectroscopy can detect structural changes produced when pendant thymine groups photo-crosslink and a cyclobutane ring is formed, via a shift in the C=O vibrational frequency towards higher wavenumbers, from 1680-1700 cm^{-1} (α,β-unsaturated amide) to 1720 cm^{-1} (α,β-saturated amide). The change in the

carbonyl stretching frequency in the IR spectra, therefore, provides information on the extent of the crosslinking reaction.

It has been reported that the major photo-products between adjacent pyrimidines upon UV excitation arise from three types of photo-reactions of the pyrimidine bases [45,46]: (1) a cyclobutane-type dimers produced by a [2π+2π] photo-cycloaddition between two C_5-C_6 double bonds; (2) a pyrimidine (6-4) pyrimidone photo-adduct involving a [2 π+2 π] addition of the C_5-C_6 double bond of the 5'-end base to the C_4-0_4 carbonyl for thymine, and (3) a nucleophilic addition of water on the C_5-C_6 double bond to give photo-hydrates. In addition, some secondary reactions of the photo-products also occur including photo-conversion of the (6-4) adducts into their Dewar valence isomers [47,48]. Besides the dimer specie, the simulated IR spectra of these species (supplementary data) do not match the experimental results, and therefore it can be conclude that the only main photo-product observed in the VBT:VBA system is the thymine photo-dimer.

On the other side, it is well known that UV light and oxygen induce reactions in polymers that cause photo-oxidative degradation and it has been extensively described in the scientific literature [49,50,51,52]. After long UV irradiation of PS, which is absorbed by the styrene chromophoric groups, various oxidation photo-products are generated and a wide variety of mechanisms can be proposed. The formation of hydroperoxides as primary photoproducts is well established. Numerous types of secondary reactions are reported that involve direct photolysis, decomposition by energy transfer, and intramolecular decomposition and lead to the formation of carbonyl and hydroxyl compound [53,54]. Aromatic and aliphatic ketones have been observed [54], and the oxidation of the aromatic ring has also been postulated. However, the main evidence for the formation of these products are the positions of the IR absorption maxima in the C=O domain.

Fig. 4a and 4b show the frequency spectra and the time profiles of each proposed species contribution for a PS sample. It can be observed the presence of the typical PS peaks around 1500 cm^{-1} due to the stretching of polystyrene aromatics at zero irradiation time, and a broad peak around 1700 cm^{-1} due to a C=O stretching in the long irradiated sample as a result of a clear photo-oxidation. The calculated IR spectra and the proposed structures are shown in Fig. 4c and 4d, respectively, and are in clear agreement with the experimental results.

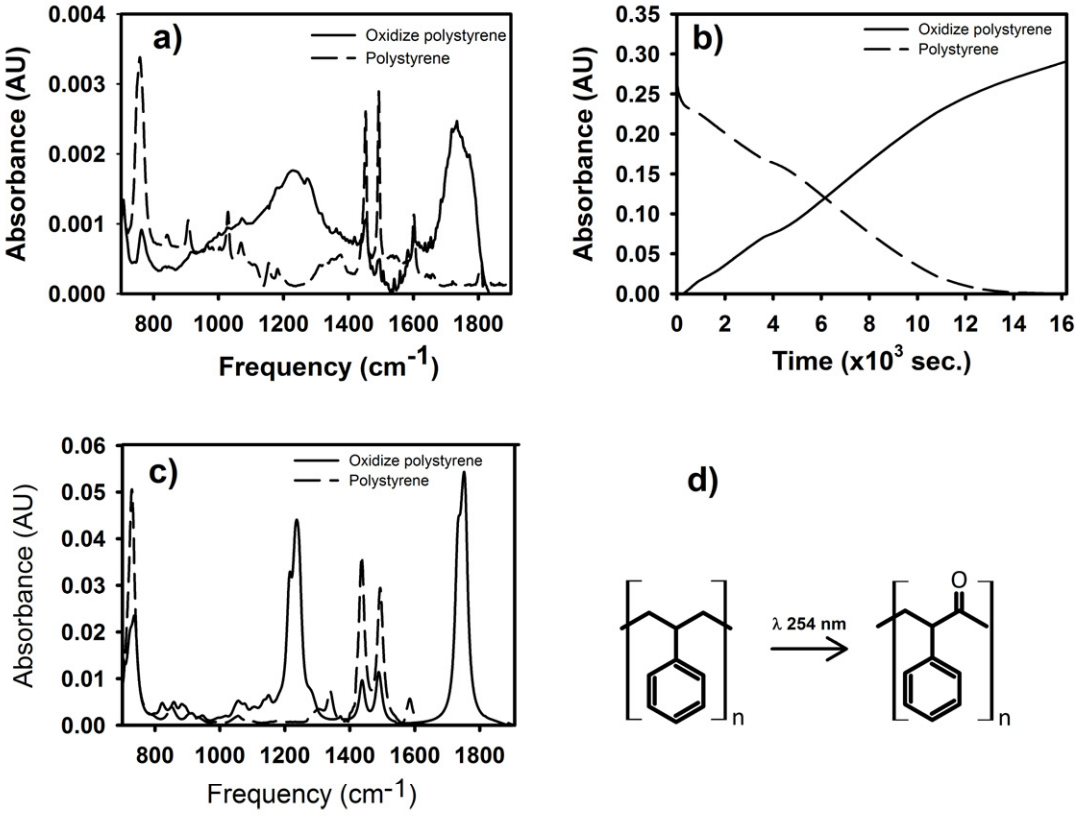

Fig. 4. a) IR signals and b) time profiles resolved by MCR-ALS for each component contribution in function of the irradiation time for PS film; c) Theoretical IR spectra and (d) proposed structures.

As a result of UV excitation of VBT:VBA polymers, besides the expected species (VBA, VBT and photo-dimer) at least one or two more photo-oxidized species may also be present. In our particular case, the photo-oxidation could occur either on the CH_2 of the VBT polymer backbone, or on the CH_2 of the VBT photo-dimer backbone. From the experimental results and the theoretical spectra (Fig. 5 and 6), the photo-product generated can be identified as the oxidized photo-dimer, since the IR peaks in the C=O domain appear at the same frequency and the main difference is a new peak at higher wavenumbers, which perfectly matches with the broadening of the experimental IR signal (Fig. 6). Another possibility is the oxidation on the CH_2 of the benzylic methylene carbon attached to thymine. The signal around 1370 cm^{-1} due to CN stretching (C* marked in Fig. 5a) would be modified, in particular enlarged and shifted towards 1360 cm^{-1}, if the CH_2 of carbon C* is replaced by the presence of C=O after photo-oxidation. However, as it will be discussed below, this possibility does not occur.

To track the crosslinking kinetics, a deconvolution of the IR spectra (700-1900 cm^{-1}) of VBT:VBA coplymer for different monomer ratios and different irradiation times was carried out using MCR-ALS. Following the algorithm explained in **Section 2.1**, four species were found to participate in the curing kinetics, namely: VBT, Photo-dimer (PD), Oxidized Photo-dimer (OP) and VBA. The calculated IR spectra and the proposed structures are presented in Fig. 5. The frequency spectra and the time profiles of each proposed species contribution for three different VBT:VBA ratios are shown in Fig. 6.

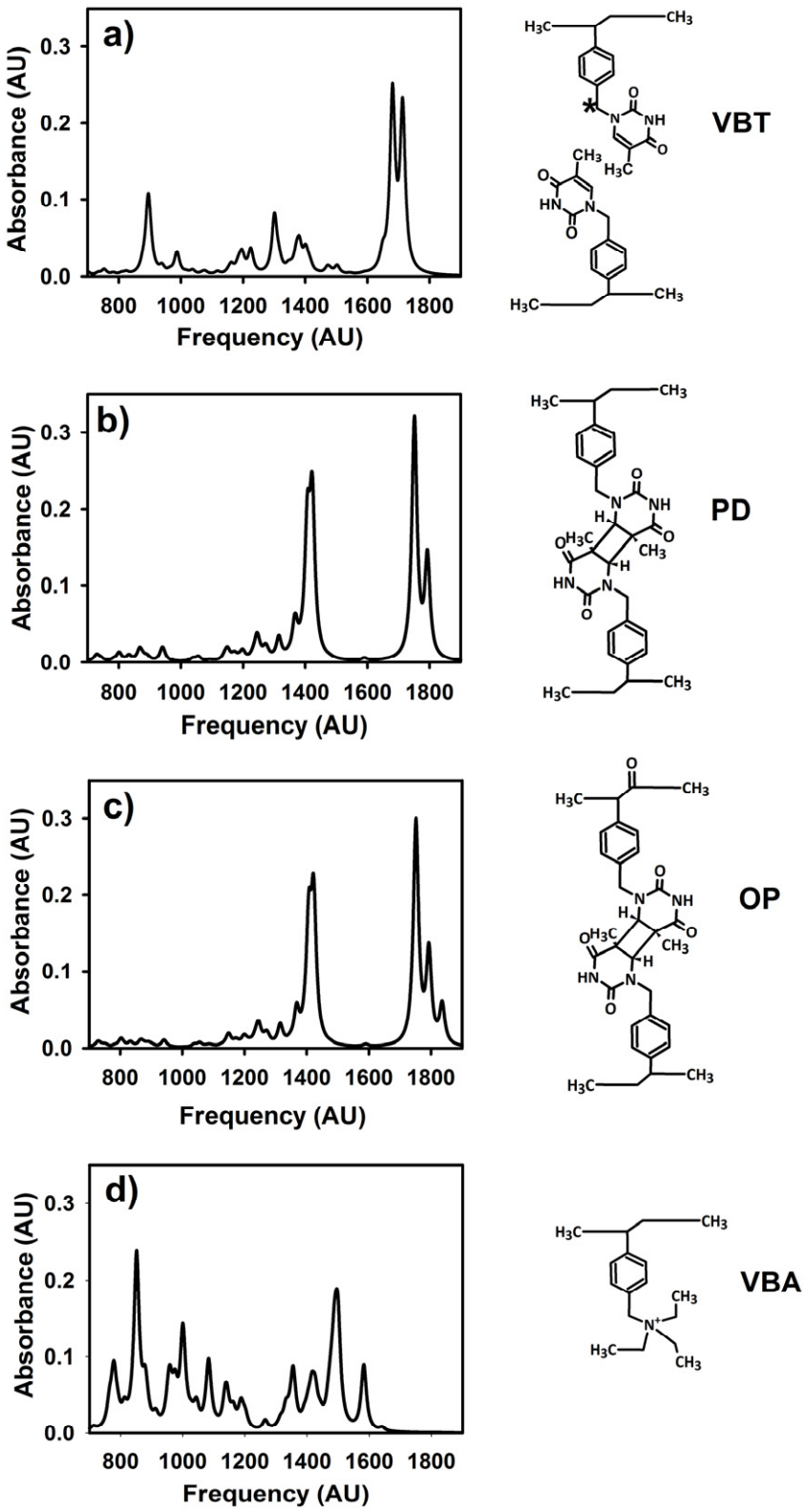

Fig. 5. Theoretical IR spectra and molecular structures for the four proposed species participating in the curing kinetics a) VBT, b) PD, c) OP and d) VBA.

Since the 5-6 carbon-carbon double bond disappears upon crosslinking, the wagging of the CH_3-C=C-H group of the thymine at 900 cm^{-1} (Fig. 5a) clearly disappears as expected in Fig.5b and 5c. Also, the theoretical spectra (Fig. 4b and 5c) demonstrate the shift of the carbonyl peaks towards higher frequencies after crosslinking, as was observed in the experimental spectra. Additionally, in the OP theoretical spectrum (Fig. 5c) the presence of a third line at higher frequencies confirms the photo-oxidation in the backbone. Finally, Fig. 5b and 5c show the presence of an intense and broad signal at ~1360-1430 cm^{-1} due to the C-N stretching of the full crosslinked thymine moieties as a result of a more rigid structure upon the curing reaction.

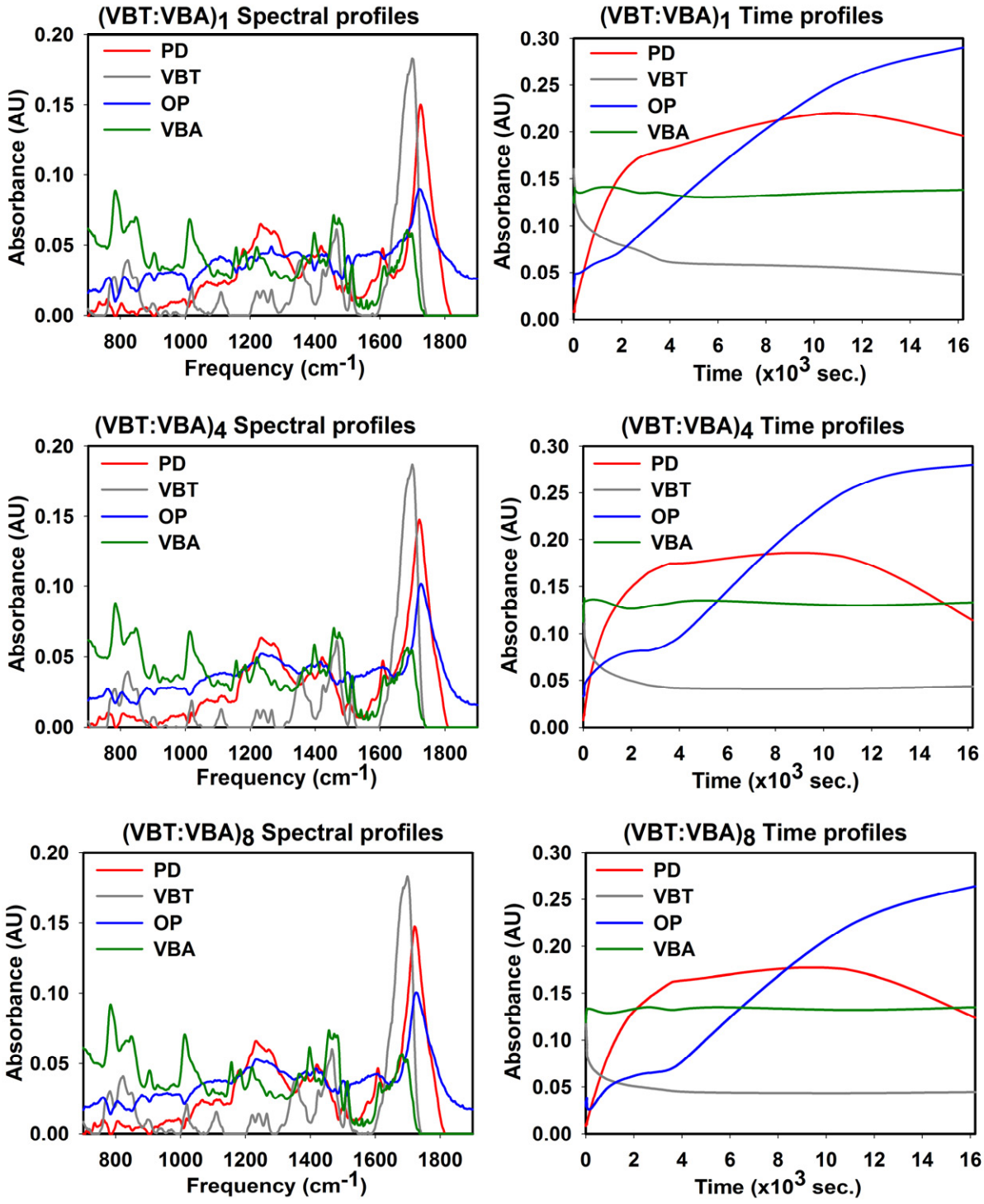

Fig. 6. Resolved IR signals and time profiles resolved by MCR-ALS for each component contribution in function of the irradiation time for three different VBT:VBA ratios.

In general, the resolved IR spectra found by MCR-ALS (Fig. 6) are quite similar to the experimental data and the theoretical output for all cases. In particular, the resolved IR signal found for VBT clearly shows the presence of the C=O vibrational frequency (1680-1700 cm^{-1}), a signal at 1490 cm^{-1} due to N-$(CH_2$-$CH_3)_3$ wagging, another one at ~ 1100 cm^{-1} corresponding to C=C-H wagging, and the aromatic CH out of plane (oop) wagging (~ 790-840 cm^{-1}), which fit quite well, both the experimental data (Fig. 3, solid line) and the theoretical spartan calculation (Fig. 5a). For all three copolymer ratios, the shift towards higher wavenumbers of the carbonyl peak of the oxidized photo-dimer OP generated after high irradiation times, is in very good agreement with the calculated theoretical spectrum (Fig. 5c), and is quite similar to the experimental spectrum shown in Fig. 3 (dashed line). Upon comparison with calculated spectrum, it is now safe to identify the oxidized species as the proposed oxidized photo-dimer OP, Fig. 5c, based on the absence of a strong signal corresponding to CN stretching (~1360 cm^{-1}) not seen in the experimental spectra.

Less straightforward is the interpretation of the other two species found by MCR-ALS. The resolved VBA spectrum presents the expected peaks due to CH oop wagging (~850 cm^{-1}), N-CH_2- wagging (~1250-1280 cm^{-1}) and N-$(CH_2$-$CH_3)_3$ wagging (~1490 cm^{-1}), while it also shows a significant difference in the region 1600-1750 cm^{-1} with respect to the theoretical spartan calculation (Fig. 5d). In addition, the resolved spectrum for the photo-dimer PD (Fig. 5b) has a structure very similar to the OP species, leading to some ambiguity in the interpretation of results. This behavior can be justified with the results presented in the previous simulated data section, where the efficiency of the algorithm was shown to decrease for systems with high spectral overlap. Nevertheless, this behavior should not preclude a satisfactory deconvolution of the experimental data.

In contrast, the resolved kinetic profiles for all species found by MCR-ALS (Fig. 6) have a good quality, and fit very well the proposed reaction mechanism (**Section 2.2**). The kinetics suggests that the VBT signal decreases as the intermediary photo-dimer PD is formed, which then disappears to yield the final oxidized photo-dimer OP. The VBA signal remains constant throughout the reaction, since the chemical environment of the VBA's cationic moieties remain unaltered after irradiation.

The results obtained with the chemometric algorithm used in this study, not only support the hypotheses concerning the proposed kinetic mechanism, but also allow the elucidation of the

oxidative photo-product formed. Additionally, once the decomposition of the total signal in the contribution of individual species is achieved, the time evolution of pure thymine concentration as a function of irradiation time can be used to characterize the kinetics of the curing process. Upcoming efforts can use these kinetic results in statistical mathematical models to simulate the crosslinking process as a function of the prepolymer molecular structure and the curing conditions.

5. CONCLUSIONS

The curing process of new materials based on styrene monomers functionalized with thymine and charged ionic groups, was studied using FT-IR spectroscopy in combination with a MCR-ALS chemometric model. A characterization of the evolution of the crosslinking process was accomplished. The curing process of the VBT-VBA copolymer was found to involve four species, which absorb in the spectral region analyzed. Furthermore, the contribution of each species to the total signal at each irradiation time was estimated. The determination of the number of species involved in the reaction process is relevant to establish the curing conditions necessary to produce a crosslinked polymer.

Additionally, the consistency of the chemometric decomposition achieved a reasonable correlation between the frequency spectra and the time evolutions obtained with the algorithm. The developed chemometric tool provided complementary information on photo-induced curing of VBT-VBA films that is crucial for developing new environmentally benign materials and new energy-saving methods. Kinetic results can be used in statistical mathematical models that simulate the crosslinking process as a function of the prepolymer molecular structure and the curing conditions. The final goal is to optimize the synthesis and curing processes to obtain materials with pre-specified properties and quality.

ACKNOWLEDGMENTS

DMM is member of the Research Council of CONICET. Authors would like to thank Universidad Nacional del Litoral (CAI+D Tipo II PI 11-57), CONICET (PIP 112-200801-01079 and D-1280/2011) and the NSF OISE (grant #1031394) for the financial support, and the W. M. Keck Foundation for funding the Undergraduate Laboratory Renaissance Program at Simmons College. Special thanks to Joe Genevich for all machining work.

REFERENCES

[1] CB Cao, C. Zhou, X. Sun, JP Gao, ZY Wang, Polymer 2010; 51: 4058-4062

[2] (a) Blackburn GM, Davies RJH. J. Chem. Soc. C 1966: 2239-2244; (b) Lamola AA, Mittal JP. Science 1966; 154: 1560-1561.

[3] Cheng CM, Egbe MI, Grasshoff JM, Guarrera DJ, Pai RP, Warner JC, Taylor LD. J. Polym. Sci., Part A: Polym. Chem. 1995; 33: 2515-2519.

[4] Grasshoff JM, Taylor LD, Warner JC. Copolymeric mordants and photographic products and processes containing same. U.S. Patent 5,395,731, March 7, 1995.

[5] Grasshoff JM, Taylor LD, Warner JC. Vinylbenzyl thymine monomers. U.S. Patent 5,455,349, October 3, 1995.

[6] Cheng CM, Egbe MI, Grasshoff JM, Guarrera DJ, Pai RP, Taylor LD, Warner JC. Proceedings of IS&T's 47th Annual Conference. The Physics and Chemistry of Imaging Systems, 1994, vol 2, pp 810.

[7] Warner JC, Morelli A, Ku MC. Methods of solubilizing and recycling biodegradable polymers containing photoreactive moieties using irradiation. U.S. 4 pp, 3,224,497, 2003.

[8] Whitfield J, Morelli A, Warner JC. J. Macromol. Sci. Part A Pure and Appl. Chem. 2005; 42: 1541-1546.

[9] El-Hayek R. Bacteriostatic Polymeric Film Immobilization. MS Thesis, UMASS, Boston, 2004.

[10] Cannon AS, Raudys J, Undurti A, Warner JC. Photoreactive Polymers and Devices for use in Hair Treatments. PCT Int. Appl., 23pp WO 2004058187 (2004)

[11] Grasshoff JM, Taylor LD, Warner JC. Method of imaging using a polymeric photoresist having pendant vinylbenzyl thymine groups. U.S. Patent 5,616,451, April 1, 1997.

[12] Grasshoff JM, Taylor LD, Warner JC. Copolymers having pendant functional thymine groups. U.S. Patent 5,708,106, January 13, 1998.

[13] Lloyd-Kindstrand L, Warner JC. In: S. Matsumura and A. Steinbüchel (Eds.) Biopolymers, vol. 9, pp 165-174, Wiley: Weinheim, Germany, 2003.

[14] Trakhtenberg S, Hangun-Balkir Y, Warner JC, Bruno FF, Kumar J, Nagarajan R, Samuelson LA. J. Am. Chem. Soc. 2005; 127: 9100-9104.

[15] Saito K, Ingalls LR, Lee J, Warner JC. Polym. Commun. 2007: 2503-2505.

[16] Saito K, Warner JC. Green Chemistry Letters and Reviews 2009; 2: 71-76.

[17] Kaur G, Chang SLY, Bell TDM, Hearn MTW, Saito KJ. Polymer Science Part A: Polymer Chemistry 2011; 49: 4121–4128.

[18] Casis N, Luciani CV, Vich Berlanga J, Estenoz DA, Martino DM, Meira GR. Green Chemistry Letters and Reviews 2007; 1: 62-75.

[19] Barbarini AL, Martino DM, Estenoz DA. Macromolecular Reaction Engineering 2010; 4: 453-460.

[20] Bortolato SA, Barbarini AL, Benitez RM, Estenoz DA, Martino DM. submitted for publication.

[21] Claybourn M, Turner P. In: Structure Properties Relations in Polymers, Advance in Chemistry Series 236, American Chemical Society: Washington, DC, 1993, pp 408.

[22] Carlson GM, Neag CM, Kuo C, Provder T. Fourier Transform Infrared Spectroscopy Characterization of Polymers, Plenem Press: New York, 1987.

[23] (a) Jenkins SL, Almond MJ, Atkinson SDM, Drew MGB, Hollins P, Mortimore JL, Tobin MJ. J. Mol. Struct. 2006; 786: 220-226; (b) Reddy AVR, Subramanian K, Sainath AVSJ. Appl. Polym. Sci. 1998; 70: 2111-2120.

[24] Hua H, Rivard T, Dubé M. Polymer 2004; 45: 345-354.

[25] Spegazzini N, Ruisánchez I, Larrechi MS. Anal. Chim. Acta 2009; 642: 155-162.

[26] De Juan A, Tauler R. Anal. Chim. Acta 2003; 500: 195-210.

[27] Olivieri AC. Anal. Chem. 2008; 80: 5713-5720.

[28] Hamerton I, Herman H, Mudhar AK, Chaplin A, Shae SJ. Polymer 2002; 43: 3381-3386.

[29] Scherzer T, Muller S, Mehnert R, Volland A, Lucht H. Polymer 2005; 46: 7072-7081.

[30] Harris DJ, Alam MK. Polymer 2002; 43: 5147-5155.

[31] Jaumot J, Gargallo R, de Juan A, Tauler R. Chemom. Intell. Lab. Syst. 2005; 76: 101-110.

[32] De Juan A, Casassas E, Tauler R. In: Encyclopedia of Analytical Chemistry; Meyers, R. A., Ed.; John Wiley & Sons, Ltd.: Chichester, U.K., 2000, pp 9800.

[33] Larrechi MS, Rius XF, Appl. Spectrosc. 2004; 58: 47-53.

[34] Garrido M, Lázaro I, Larrechi MS, Rius FX. Anal. Chim. Acta 2004; 515: 65-73.

[35] Garrido M, Larrechi MS, Rius FX. Anal. Chim. Acta 2007; 585: 277-285.

[36] Garrido M, Rius FX, Larrechi MS. Anal. Bioanal. Chem. 2008; 390: 2059-2066.

[37] Jaumot J, Vives M, Gargallo R, Tauler R. Anal. Chim. Acta 2003; 490: 253-264.

[38] Maeder M, Zilian A. Chemom. Intell. Lab. Syst. 1988; 3: 205-213.

[39] Windig W, Guilment J. Anal. Chem. 1991; 63: 1425-1432.

[40] MacLeod DM. In: Coating Technology Handbook, D. Satas, Ed.; Marcel Dekker: New York, 1991.

[41] Pike Technologies, Inc. Measurement of Monomolecular Layers using Specialized FTIR Grazing Angle Accessories; Specular Reflectance - Theory and Applications., 2005.

[42] MATLAB 7.0, The Mathworks, Natick, Massachussets, USA, 2007.

[43] http://www.ub.es/gesq/mcr/mcr.htm.

[44] SPARTAN'08, Wavefunction Inc., Irvine, California, USA, 2009.

[45] Lemaire DGE, Ruzsicska BP. Photochem. Photobiol. 1993; 57(5): 755-769.

[46] Douki T, Zalizniak T, Cadet J. Photochem. Photobiol. 1997; 66(2): 171-179

[47] Douki T, Voituriez L, Cadet J. Photochem. Photobiol. 1991; 53: 293-297

[48] Taylor J S, Lu HF. Photochem. Photobiol. 1990; 51: 161-167.

[49] Lucas PC, Porter RS. Polym. Degrad. Stab. 1985; 13(4): 287-295.

[50] Mailhot B, Gardette JL. Macromolecules 1992; 25: 4127-4133.

[51] Mailhot B, Gardette JL. Macromolecules 1992; 25: 4119-4126.

[52] Mailhot B, Jarroux N, Gardette JL. Polym. Degrad. Stab. 2000; 68: 321-326.

[53] Lucas PC, Porter RS. Polym. Degrad. Stab. 1989; 26: 203.

[54] Geuakens G, Baeyens-Volant D, Delaunois G, Lu-Vinh Q, Piret W, David C. Eur. Polym. J. 1978; 14: 291.